size of the modern cormorant *Phalacrocorax penicillatus* (*1*). Other species were only slightly smaller than the largest living penguins, and two species far exceeded existing penguins in size. In life, the largest Japanese plotopterid (see cover) probably measured more than 2 m from bill tip to tail tip and may have been larger (*4*) than any of the giant fossil penguins from the Tertiary of the Southern Hemisphere (*5*).

The most striking feature of the Plotopteridae is the wing, which had lost all resemblance to that in other Pelecaniformes and was modified as a rigid paddle, unsuitable for flight. The wing bones show numerous parallels with those of penguins and the flightless Alcidae (Fig. 1). The head of the humerus is heavy, nearly spherical, and penguinlike, whereas the distal end of the humerus and the elongated first metacarpal more closely resemble those of flightless auks. A row of distinct pits on the dorsal surface of the ulna is unique; in most birds the secondaries attach to raised papillae. The articulating surfaces of the wrist bones indicate that the hand was capable of very little flexion (*3*).

As in penguins, the scapula was greatly expanded to provide increased attachment for the muscles used to raise the wing against water, a much denser medium than air. Also as in penguins, the limb bones were extremely dense and heavy, serving to reduce buoyancy.

Despite the great modification of the wing and scapula, the remainder of the skeleton in the Plotopteridae shows close affinity with the Pelecaniformes. The carina of the sternum articulates solidly with the furcula, there is a very large acromion process of the scapula, and the skull has a deep, transverse nasofrontal hinge and lacks supraorbital impressions for salt glands. These characteristic features of the Pelecaniformes are not found in penguins or auks. The tarsometatarsus, although quite robust, is most like that of anhingas and has little resemblance to that of penguins, in which, for example, the metatarsals are incompletely fused (Fig. 2).

In much of the skeleton of the Plotopteridae, the greatest similarity is to anhingas, which otherwise differ considerably in being freshwater, foot-propelled diving birds with the head and neck highly modified as a spearing device. Such specializations of the head and neck are absent in the Plotopteridae, however, and the skull is more like that in the Sulidae (gannets and boobies).

Adaptations for the use of the wings rather than the feet in underwater propulsion have evolved in several groups of birds. The penguins are so modified to this end that their ancestry is no longer readily discernible. Nevertheless, despite earlier opinions to the contrary, they are now generally regarded as having descended from volant ancestors (*6*). The convergent adaptations of the Plotopteridae offer significant proof that almost any group of water birds could evolve an essentially penguinlike morphology in becoming specialized for wing-propelled diving.

Storer (*6*) remarked on the absence in the Northern Hemisphere of wing-propelled diving birds of the size of the larger Recent penguins or their giant fossil relatives. We now know, however, that the Plotopteridae occupied such niches in the North Pacific for an undetermined period prior to the end of the early Miocene. Plotopterids are not known from the more intensively studied younger deposits around the North Pacific, and it seems likely that they became extinct at the same time as the giant penguins in the Southern Hemisphere. Simpson (*5*) has suggested that niches for pelagic endotherms the size of giant penguins may have been preempted by seals and porpoises, which underwent their greatest diversification during the Miocene. Because plotopterids occupied niches similar to those of giant penguins but are unrelated and occurred in a different hemisphere, their simultaneous disappearance adds considerable support to Simpson's hypothesis. In addition, the Plotopteridae provide one of the more impressive instances of convergent evolution in the fossil record.

STORRS L. OLSON
Department of Vertebrate Zoology,
National Museum of Natural History,
Smithsonian Institution,
Washington, D.C. 20560

YOSHIKAZU HASEGAWA
National Science Museum,
Tokyo 160, Japan

References and Notes

1. H. Howard, *Condor* **71**, 68 (1969).
2. The Washington specimen is from the Pysht Formation, Twin River Group. Japanese specimens are from the Asagai, Ashiya, Hatazu, and Nishisonogi formations [see Y. Hasegawa, *Proc. 1st Int. Congr. Pac. Neogene Stratigr.* (1977), p. 340; *Kagaku Asahi* **3**, 71 (1978); *Bull. Kita Kyushu Mus. Nat. Hist.* **1**, 41 (1979)].
3. S. Olson, *Nat. Hist. Mus. Los Angeles Cty. Contrib. Sci.*, in press.
4. The length of a recently collected synsacrum of *Anthropornis nordenskjoeldii*, the largest or next to largest of the giant fossil penguins, is 240 mm, whereas that in the largest Japanese plotopterid is approximately 330 mm.
5. G. Simpson, in *The Biology of Penguins*, B. Stonehouse, Ed. (Macmillan, London, 1974), pp. 30–32.
6. R. Storer, *Proc. 12th Int. Ornithol. Congr.* (1960), p. 694.
7. For collecting, preparing, or providing information on specimens we thank U. Akagi, H. Endo, D. Emlong, S. Isotani, K. Isozaki, Kita Kyusyu Natural History Museum, H. Kodama, K. Matsuo, J. Mori, S. Ota, H. Otsuka, C. Ray, K. Seki, G. Sullivan, Y. Suyana, T. Suzuki, and W. Zinsmeister. Illustrations are by B. Dalzell. J. Farrand, C. Ray, and D. Steadman commented on the manuscript.

13 April 1979; revised 14 May 1979

Angular Invariants in Developing Human Mandibles

Abstract. *Recent studies of lateral cephalograms based on symmetric-axis analyses of the mandibular border yield angles that appear to be uninfluenced by gross changes in mandibular shape over age and between individuals.*

The symmetric axis of an outline form is a curve passing down a precisely defined middle of an extended structure. This curve plus an expression of its distance from the boundary is sufficient to completely describe the shape of the structure. Rigorous definitions and theorems have been published (*1, 2*). These axes can provide stick figures for complex biological forms, which serve as a means for registering slow changes in curvature, relative position of parts, and so forth, for organs assembled out of poorly delimited parts. In this report we show that symmetric axes derived from lateral projections of the human mandible obtained serially from cephalograms of normal and aberrant individuals define remarkably stable angles.

Figure 1 shows the symmetric axis defined by a mandibular shape. It may be considered the locus of centers of "max-

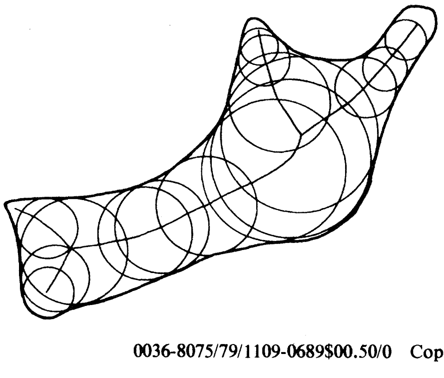

Fig. 1. Lateral projection of human mandibular border showing representative maximal disks whose loci of centers determine the symmetric axis. Radii of disks are expressed as functions of distance along the symmetric axis and determine the radius function, which, along with the loci of centers, provides a complete description of the shape of the mandibular border.

imal disks" that lie completely within the closed border. When such a disk touches the boundary in more than two discrete places it defines a branch point. One such branch is located in the ramus and another in the anterior portion of the body (Fig. 1). The angles determined by such branches in a homologous series can be compared visually by superimposing corresponding branch points and rotating the axis segments for best fit.

Data on cephalometric axes can be superposed at the ramus branch point obtained from two different sources. Figure 2A shows nine Broadbent-Bolton standards, and Fig. 2B shows these standards in register with data obtained from two dysostotic individuals at various ages. [The Broadbent-Bolton cephalometric standards are a graphic abstraction of thousands of children ranging in age from 1 to 18 (*3*).] Conventions used to approximate the shape of the alveolar process and the tip of the condyle from missing data in the Broadbent-Bolton series do not influence the conclusions drawn in this report since only well defined portions of the mandibular boundary are responsible for the shape of the symmetric axis near the angles described. Hence, they contain shape information derived from a large base of longitudinally and cross-sectionally obtained cephalometric data. The symmetric axes of mandibular outlines traced from these standards were calculated and plotted with a computer program that transforms a digitized representation of the mandibular border into its symmetric-axis coordinates in real space. This analysis was performed on 9 of the 18 standards, starting at 1 year of age and taking each odd year through age 17. The digitized images were tested vertically and horizontally for errors in magnification. They were found to be uniform to within 0.5 mm relative to the originals.

Notice that all axis segments (Fig. 2A) near the triple point can be superimposed almost perfectly. The circular inset gives a more accurate and enlarged view of the superimposed branches showing the discrete points determined by the computer analysis. The mean angles of 140°, 130°, and 90° were determined from visual inspection. They are the limiting tangents to curving axis segments at the branch based on estimates obtained for each age independently. The respective standard deviations are 3°, 2° and 2°, with maximum deviations not exceeding 4°. The degree of axial congruity is more precise than these absolute angular estimates indicate (Fig. 2A, inset), suggesting that much of the observed variation may be attributed to arbitrary judgments inherent in fitting tangents to discrete points on curving axes. The additional symmetric axes (Fig. 2B) were derived from the rami of two persons suffering from untreated mandibulofacial dysostosis (Treacher-Collins syndrome). These mandibles are characterized by extreme variation and grossly abnormal shape (*4*); hence they provide a stringent test for variation both within and between individuals. Patients 1 and 2 were studied at ages 4, 9, and 14 years and 6, 8, 10, and 12 years, respectively. In each case the angle determined by the axis segment associated with the lower portion of the condyle near the triple point appears constant (Fig. 2B); the angles are superimposed to the accuracy of the measurements. The angles determined by the axis segment produced by the coronoid do not share this age independence in patient 1, but do seem relatively independent of age in patient 2.

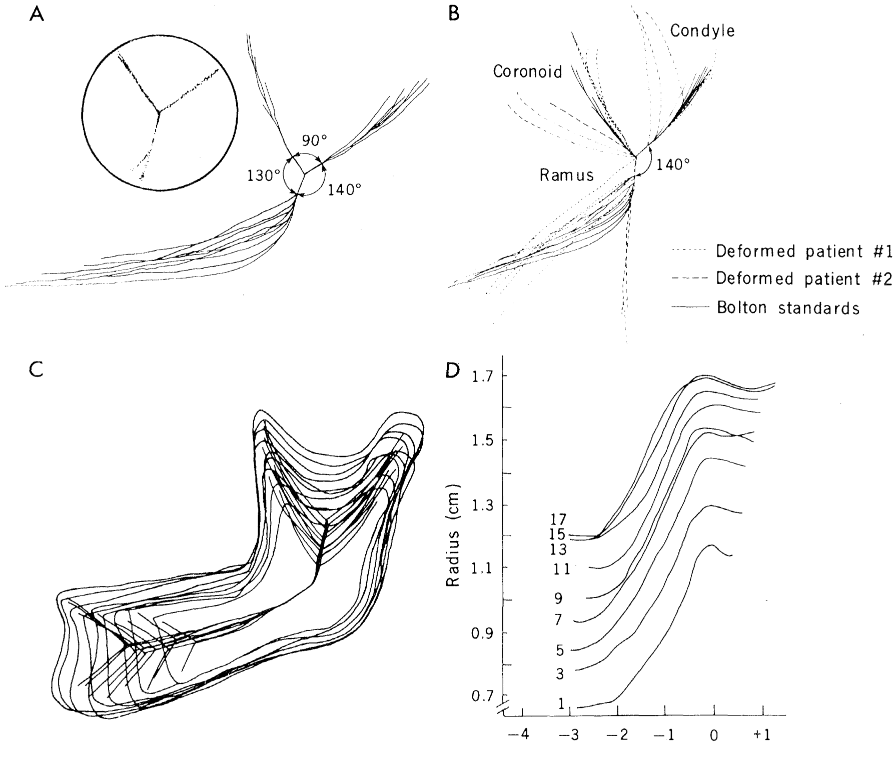

Fig. 2. Composite overlay of symmetric axes near the superior triple point. (A) Axes derived from nine Broadbent-Bolton standards. The circular inset shows an enlarged, more accurate view of the superimposed branches near the triple point. (B) The same standards plus axes from longitudinal cephalograms of two different dysostotic individuals. Gonial branches have been deleted for clarity. (C) Composite overlay of symmetric axes corresponding to the gonial region of the Broadbent-Bolton standards. Axes are coincident at point of maximum curvature and rotated for best fit. (D) Corresponding gonial radius functions. The identifying numbers refer to the age of each standard. The curves are aligned such that the points determined by the region of maximum curvature on the symmetric axes have the same abscissa.

De Souza and Houghton were among the first to apply symmetric-axis analysis to the study of biological shape (*5*). Their paper contains a single symmetric axis derived from an unusual Polynesian mandible called a "rocker-jaw." When we superimposed these same angles of 140°, 130°, and 90° with the homologous triple-point angles computed independently by de Souza and Houghton, we found the fit to be indistinguishable from that in Fig. 2A.

A similar analysis on the Broadbent-Bolton series was done for the symmetric axis determined by the gonial region. The symmetric-axis analogs of the respective gonial angles were overlaid by superposing the points of maximum curvature and rotating for best fit (Fig. 2C). These "angles" do not come to a corner and hence are not angles in the conventional geometric sense. Again, the shape of the symmetric axes appears relatively constant and independent of age, within the accuracy of measurement (*6*).

Figure 2D shows the radius functions associated with these angles. These functions approach simple vertical displacements of each other where they exist, which means that the upper and lower mandibular boundaries described by homologous parts of respective symmetric axes are nearly parallel in this region. Gross anatomic variations in the dysostotic mandibles preclude a simple analysis of this type for these data.

Considered in toto, these data confirm that symmetric-axis analysis can be used (i) to quantify shape properties of the human mandible, (ii) to make longitudinal comparisons of shape of individuals having specified developmental anomalies, and (iii) to determine angular invariants in the lateral shape of the human mandible, some of which appear to be relatively independent of age both within and between individuals.

The mechanism responsible for these findings is unknown. Some investigators hold that skeletal development is regulated largely by genetic determinants, while others believe that the play of mechanical stresses is the dominant influence (7). More likely both mechanisms interplay in a complex fashion. The remarkable stability of these angles with age suggests that they may correspond to genetically influenced discontinuities analogous to branches of a tree near their origin. Bifurcation angles are relatively independent of age, even though the direction a branch may take shortly after division is heavily influenced by a host of environmental factors. If this analogy holds, we would expect analysis of branch points and symmetric-axis angles in other skeletal systems amenable to accurate registration in two dimensions to yield comparable findings.

RICHARD L. WEBBER
National Institute of Dental Research,
National Institutes of Health,
Bethesda, Maryland 20014

HARRY BLUM
Division of Computer Research
and Technology,
National Institutes of Health

References and Notes

1. H. Blum, *Ann. N.Y. Acad. Sci.* **231**, 19 (1974); *J. Theor. Biol.* **38**, 205 (1973).
2. _____ and R. Nagel, *Pattern Recognition* **10**, 167 (1978).
3. B. H. Broadbent, Sr., B. H. Broadbent, Jr., W. H. Golden, *Bolton Standards of Dentofacial Developmental Growth* (Mosby, St. Louis, 1975).
4. F. G. Roberts, S. Pruzansky, H. Aduss, *Arch. Oral Biol.* **20**, 265 (1975); S. Pruzansky, *Birth Defects Orig. Artic. Ser.* **5**, 120 (1969).
5. P. V. de Souza and P. Houghton, *Comp. Biomed. Res.* **10**, 333 (1977).
6. R. L. Webber, H. Blum, R. N. Nagel, *Int. Assoc. Dent. Res. Abstr.* **57**, 112 (1978).
7. D. H. Enlow, *Handbook of Facial Growth* (Saunders, Philadelphia, 1975).
8. We thank R. N. Nagel, M. O'Conner, and M. Nashman for the computer implementation of this project; R. Christiansen, S. Pruzanski, and H. Aduss for the cephalometric data evaluated in this study; and J. Mosimann for his guidance and helpful editorial suggestions.

10 May 1979; revised 11 July 1979

A New Mineralized Layer in the Hinge of the Oyster

Abstract. *A discrete, calcareous layer that binds the foliated calcite of the oyster's shell to the organic ligament in the hinge is reported, apparently for the first time. This layer is ultrastructurally, and generally mineralogically, different from the underlying foliated calcite, and is named the ligostracum.*

In molluscan bivalves, a thin, discrete, mineralized veneer that is continuous over the outer surface of the valves binds the organic periostracum to the outermost mineralized shell region. This layer, the mosaicostracum, has been described ultrastructurally in tellinid bivalves (*1*) and in the blue mussel *Mytilus edulis* (*2*), and is homologous with a similar layer on the surface of the valves of gastropods (*3*).

The juncture between the mineralized shell and the ligament in bivalves has apparently not been investigated. We report the presence of a thin, distinct, calcareous layer in the hinge of oysters that binds the foliated calcite of the shell in the umbonal region to the organic ligament. We name this layer the ligostracum (L., *ligare*, to bind; Gk., *ostrakon*, shell). It is ultrastructurally, and generally mineralogically, different from the underlying foliated calcite of the shell.

We examined 12 *Crassostrea virginica* oysters. Some came from an estuary in Delaware, some from local controlled maricultural systems (*4*), and others from Florida. They ranged in height from 1.7 to 6.0 cm. We also studied adult specimens of *C. angulata*, *C. gigas*, *Ostrea edulis*, *O. lurida*, and *O. equestris* (Table 1). The umbonal region of each oyster shell was removed with a diamond saw and the ligament was dissolved in sodium hypochlorite (0.5 to 1.8 percent) for 15 to 48 hours at room temperature. Time of immersion and concentration of sodium hypochlorite were determined by shell size. Chondrophoral and nymphal surfaces (Fig. 1, A and B) (*5*) of the hinge on right and left valves were brushed clean with a soft brush, rinsed, and dried. Differentiation of calcite and aragonite was accomplished with Feigl's stain (10 to 30 minutes) rather than with x-ray diffraction because of the thinness of the ligostracum (*6*). Umbonal shell pieces were mounted with silver paint onto aluminum stubs, freeze-dried for 4 days, coated in vacuum with carbon and gold, and then studied with a scanning electron microscope (Philips 501).

Chondrophoral and nymphal surfaces of the hinge of the right valve (Fig. 1B) in all of the oysters we examined were distinctly aragonitic, staining intensely black with Feigl's fluid. However, on the left (attached) valve (Fig. 1A), chondrophoral and nymphal areas were aragonitic only in *O. lurida* and *O. equestris* (Table 1). In the other species the two minerals were heterogeneously distributed on these surfaces. The presence of two $CaCO_3$ polymorphs in a single shell layer is rare in the Bivalvia (*7*). Mixed polymorphs of $CaCO_3$ were also found in other areas of the valves. For example, sawed cross sections of the umbonal region of the valves disclosed prominent strata of aragonite alternating with strata of calcite in *C. virginica* and *C. gigas* and traces of aragonitic strata in the other four species—an observation which may not have been made before for ostreids (*8*). Although artifacts with Feigl's stain are possible (*9*), the intensity and rapidity of the staining tend to confirm the aragonitic nature of these strata. This suggests that the oysters, in response to environmental or physiological changes,

Table 1. Mineralogy of the ligostracum of the left valve in various oysters. The chondrophores and nymphae of the right valve contained aragonite in each case.

Species	Source	Chondrophores	Nymphae
Crassostrea virginica (Gmelin)	Delaware Florida	Calcite with traces of aragonite	Calcite with traces of aragonite
Crassostrea angulata (Lamarck)	England	Aragonite with traces of calcite	Aragonite
Crassostrea gigas (Thunberg)	Washington	Aragonite and calcite mixed	Aragonite with traces of calcite
Ostrea edulis (Linné)	Maine	Aragonite and calcite mixed	Aragonite
Ostrea lurida (Carpenter)	Washington	Aragonite	Aragonite
Ostrea equestris (Say)	North Carolina	Aragonite	Aragonite

0036-8075/79/1109-0691$00.50/0